JOURNAL OF SOLID STATE CHEMISTRY 106, 219–236 (1993)

Solid Phase Transitions and Fast Ion Transport in $LiNaSO_4 : LiCl : Na_2WO_4$ Mixed Systems*

S. R. SAHAYA PRABAHARAN†‡ AND P. MUTHUSUBRAMANIAN

Materials Science Laboratory, School of Energy Sciences, Madurai Kamaraj University, Madurai 625 021, India

AND M. ANBU KULANDAINATHAN AND V. KAPALI

Central Electro-chemical Research Institute, Karaikudi 623 006, India

Received February 19, 1992; in revised form December 29, 1992; accepted December 29, 1992

$LiNaSO_4 : LiCl : Na_2WO_4$ composites of a few different compositions have been prepared by quenching the melt and studied for the first time with a view to improve the ionic conductivity of $LiNaSO_4$ at the lowest possible temperature. The phase formations of the composites have been analyzed by means of X-ray powder diffraction technique. The transport properties have been studied by DSC and complex ac impedance analysis (to extract the dc electrical conductivity, σ_{dc}). The X-ray diffractograms show evidence for solid solutions (ss) as well as a second dispersed phase due to undissolved excess compound (LiCl). The σ enhancement may be attributed to the increase in interfacial conductivity due to the increase in concentration of the charge carriers (ions or vacancies) forming a diffuse space charge layer between the two ion conductors, i.e., the solid solution of $LiNaSO_4$ with dissolved chloride and tungstate fractions and a chloride phase with dissolved sulfate fraction. DSC measurements show improved thermal properties with respect to α-$LiNaSO_4$. The present composite mixtures offer the choice of lower transition temperatures, but these are accompanied by lower transition enthalpies.

Introduction

Because of the great technological incentives for the development of more effective and efficient ways of converting and storing energy, much of the attention being given to fast-ion conductors or solid electrolytes at the present time is either directly or indirectly related to their potential use in new types of batteries (the so-called solid state batteries) and fuel cells for power source applications. The current abiding interest in solid electrolytes as demonstrated by the large number of books and reviews (*1–6*) is mainly a result of the potential applications of these materials in ion-selective electrodes, capacitors, gas sensors, electrochromic display devices, high-temperature heating elements, intercalation electrodes, etc. The possible applications of solid ionic materials for batteries have recently been reviewed (*7*). Interest in studying fast-ion conductors arises not only from the great variety of technological applications in which they are involved, but also from the fundamental need to understand the fast-

* Part of the results presented in this paper was accepted for presentation at the 8th International Conference on Solid State Ionics, Lake Louise, Alberta, Canada, 1992; Extended Abstract, paper XO8 (1992).

† To whom correspondence should be addressed at Central Electrochemical Research Institute, Karaikudi 623 006, India.

‡ Research contained in this paper was performed for partial fulfilment of the Ph.D. requirements in Physical Sciences at Madurai Kamaraj University, India (1992).

0022-4596/93 $5.00

ionic behavior and, possibly, thereby improve the properties of such compounds (*8–10*).

In this context, considerable effort is being made to develop good Li^+-ion based solid electrolytes, suitable for solid state battery applications. Extensive studies have been conducted on a number of lithium-based solid electrolytes and of these Li_2SO_4-based compounds are important (*11–16*). Nevertheless, all the efforts have failed to stabilize the high conducting Li_2SO_4 phase (fcc) at or near the room temperature, although the fast-ion conducting transition temperature (T_t) could be lowered by as much as 100°C by the addition of other mono- and divalent cations such as Na^+, Ag^+, Zn^{++}, etc. The family of mixed binary sulfates of the $LiM'SO_4$ (M' = Na, Ag, NH_4, Zn, . . .) type possesses interesting electrical transport properties.

Investigations have been continuing in various aspects on equimolar binary $LiNaSO_4$ since 1958. Lithium sulfate and sodium sulfate are two interesting salts for which quite a number of investigations have been made. According to the binary phase diagram for the system, Li_2SO_4–Na_2SO_4, the intermediate phase, β-$LiNaSO_4$, is stable within a narrow concentration range (*17, 18*). The structure at this phase has been claimed to be trigonal with space group $P31C$ (*19, 20*). Venudhar *et al.* studied the temperature dependence of the lattice parameters of the trigonal phase of $LiNaSO_4$ (*21*), and they report that the diffraction patterns were not measurable at 470 and 510°C and that the pattern taken at about 560°C was completely different from those at lower temperatures. The high-temperature phase of $LiNaSO_4$ has been described as a plastic phase (*22*), that is, a phase characterized by extensive orientational disorder of the sulfate ions (*23*). The structure of the high-temperature phase was determined by Förland and Krogh-Moe (*24*). For the equimolar composition the phase transition occurs at 518°C from trigonal to bcc with 155 kJ/kg latent heat of transformation and the salt melts at 615°C. A comparison of all these properties of both low and high temperature phases of equimolar-$LiNaSO_4$ has recently been reported (*25*).

The NMR results (*26*) seem to contradict the β-phase (trigonal with space group $P31C$), but the results of an extensive high-resolution neutron diffraction study (*27*) only allow small deviations from the originally suggested structure. Recently, Massiot *et al.* (*28*) studied both low- and high-temperature phases of $LiNaSO_4$ by means of a high-temperature NMR probe and they proposed a double resonance mechanism between cations (Li^+ and Na^+) jumps and SO_4 rotations at the solid–solid phase transformation. Furthermore, the high-temperature neutron powder diffraction study of α-$LiNaSO_4$ shows that the Li^+-ions are in tetrahedral positions whereas, the Na^+-ions are in octahedral sites (*29*), and this suggests that the migration of the two cation species (Li^+ and Na^+) in bcc-$LiNaSO_4$ should not be strongly correlated. This observation has subsequently been confirmed from the results of high-temperature neutron study using single crystal Li_2SO_4 (*30*).

In α-$LiNaSO_4$, the diffusion coefficients for Li^+ and Na^+ are almost equal (D_{Li^+} = 1.00×10^{-5} cm^2/sec; $D_{Na^+} = 0.93 \times 10^{-5}$ cm^2/sec at 550°) (*31*). The ionic conductivity of low-temperature β-$LiNaSO_4$ is low (*32–34*). Mellander *et al.* (*35*) have recently studied the ion transport properties of single crystal $LiNaSO_4$ within the β-phase by means of impedance spectroscopy. The high-temperature bcc phase has quite remarkable properties. The electrical conductivity is 0.92 S/cm at 550°C (*13, 32*). But, according to our reinvestigation results (*36*), the high-temperature electrical as well as thermal properties differ considerably (see elsewhere in this article). Just below the melting point the conductivity is 1.35 S/cm and it increases by about 10% when the salt melts. These results are in at least qualitative agreement with several studies of the system Li_2SO_4–Na_2SO_4 (*33, 34*). Thus, the electrical properties of the bcc phase are

characteristic of a solid electrolyte (or fast-ion conductor), while the rheological properties and the large latent heat of the solid–solid transition are typical for a plastic crystal. The high conductivity phase is described as "rotator phase" and the enhanced cation mobility is attributed strongly to the coupled rotational motion of translationally static SO_4 ions on the basis of the so-called "paddle-wheel" mechanism (*37*). It is worth mentioning the existing controversy between Lundén (*37*) and Secco (*38*) in this regard.

The structural and dynamical behavior of $LiNaSO_4$ compound both in low- and high-temperature ranges have also been studied by different spectroscopic techniques such as IR reflectivity (*39*) and Raman scattering (*40–43*).

Whereas, this paper reports the first results obtained on the effect of simultaneous additions of both alio-(LiCl) and iso-(Na_2WO_4) valent guest anions into equimolar-$LiNaSO_4$ binary system. A similar study with Na_2MoO_4 instead of Na_2WO_4 has been published elsewhere (*44*).

Experimental

Starting materials, $Li_2SO_4 \cdot H_2O$ (suprapure) and Na_2SO_4, were obtained from SISCO (India) and LiCl and $Na_2WO_4 \cdot 2H_2O$ were supplied by E. Merck Ltd. (India). All chemicals used in this study were analytical reagent quality grade. The quenched product in each composition appeared as a solid solution and/or two- or multiphase mixtures and confirmed by XRD and DSC effects.

Prior to the preparation of the present composites, the additives LiCl and $Na_2WO_4 \cdot 2H_2O$ were initially dried at 150°C. The polycrystalline $LiNaSO_4$ was taken as a bulk parent and LiCl and Na_2WO_4 were added in various mole fractions to get the composite mixtures. The studied compositions ($LiNaSO_4$: LiCl : Na_2WO_4) were prepared in the following mole fractions, i.e., 90 : 10 : 0, 90 : 9 : 1, 90 : 7 : 3, 90 : 5 : 5, 90 : 3 : 7, and 90 : 0 : 10. All these mixtures were initially ground together and subsequently melted in air. The melts were then quenched to room temperature on to a clean aluminium sheet under a water bath in order to increase the rate of quenching. The resolidified masses were finely ground to get a fine powder. All the samples were dried for 15 hr at 150°C before various measurements were made.

The phase analysis of these composite mixtures was made with XRD using Cu$K\alpha$ radiation (JEOL, JDX 8030, X-ray diffractometer, Japan) at room temperature.

The DSC traces were obtained with a SHIMADZU DSC 50 thermal analyzer equipped with disk memory. The samples were typically around 11 mg and were put in an aluminum sample crucible in a flowing argon atmosphere (30 ml/min). The transition temperature T_t and transition enthalpy ΔH_t (kJ/kg) were obtained on samples up to 560°C with a constant heating rate of 10°C/min.

The conductivity measurements were carried out with pellets obtained by pressing the fine powdered samples under the pressure of 5 tons/cm^2 using a stainless steel die and a hand-operated hydraulic press. The thickness of the pellets were ~3.5 mm with the diameter of 14.5 mm. To minimize the electrical contact problems, the flat faces of the pellets were coated with quick drying graphite aquadag (Dag #154, Acheson, Holland) on both sides as electrodes. Such pellets were then stacked between platinum electrodes in order to ensure proper electrical contact. A home designed spring loaded stainless steel conductivity cell was used for electrical measurements which could be inserted inside a cylindrical tube furnace (Heraeus, Germany) whose temperature was controlled and measured to within 3°C. The resistance of the electrode leads was less than 1 ohm and was too small to influence the impedance data.

For electrical conductivity measurements an ac-impedance technique was employed using a Solartron 1250/1286 FRA set up (between 10 Hz and 65 kHz) as a function of

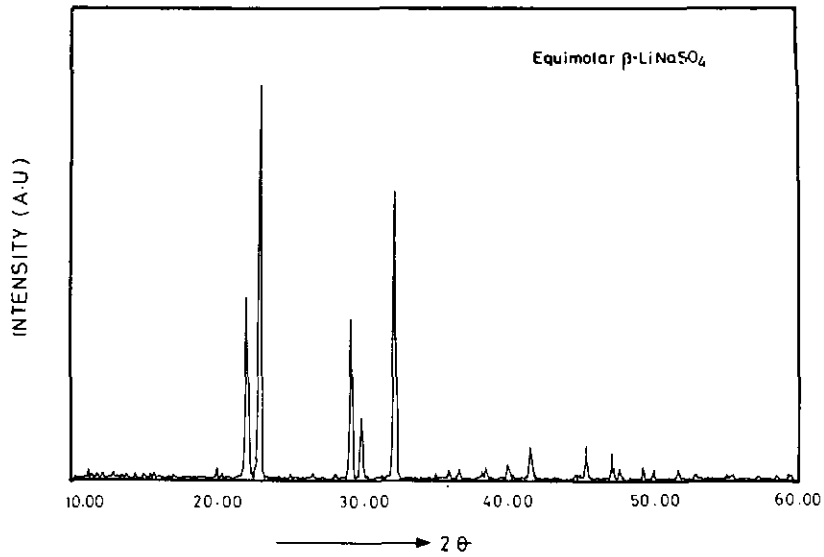

FIG. 1. X-ray powder diffractogram of equimolar-$LiNaSO_4$ at room temperature (30°C).

temperature with applied nominal voltage of 20 mV. Grain boundary impedances were minimized by attention to firing condition for the pellets and all the conductivity data reported are bulk conductivity values. Prior to each set of measurements, the conductivity cell was allowed to equilibrate at the temperature of the furnace for 30 min. Measurements were made, isothermally, on heating cycle only. The temperature range covered was 350–545°C.

Results and Discussion

1. X-Ray Analysis

The X-ray diffractograms for different mixtures of various mole fractions of $LiNaSO_4 : LiCl : Na_2WO_4$ and also their binary end members, $LiNaSO_4 : LiCl$ (90 : 10 mole%) and $LiNaSO_4 : Na_2WO_4$ (90 : 10 mole%), are shown in Fig. 2. The XRD diffractograms corresponding to the binary reciprocal salt systems $LiNaSO_4 : LiCl$ (90 : 10 mole%) and $LiNaSO_4 : Na_2WO_4$ (90 : 10 mole%), and $LiNaSO_4 : LiCl : Na_2WO_4$ composites with different mole compositions (90 : 9 : 1, 90 : 7 : 3, 90 : 5 : 5, and 90 : 3 : 7) exhibit features typical to that of β-$LiNaSO_4$

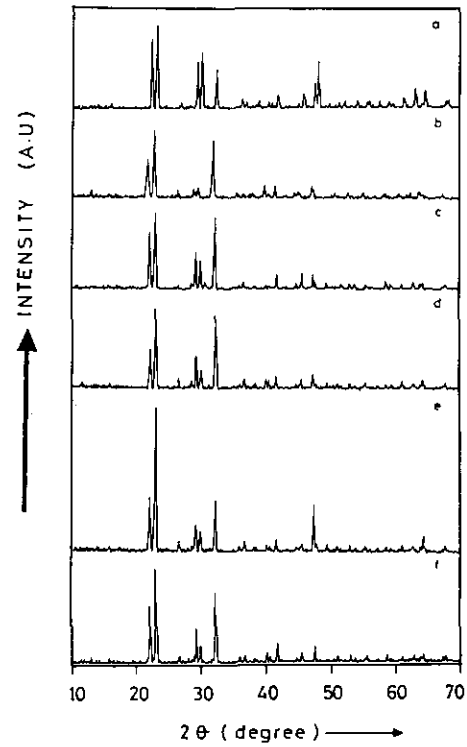

FIG. 2. X-ray powder diffractograms of mixtures of $LiNaSO_4 : LiCl : Na_2WO_4$ mixed systems in the following mole compositions; (a) (90 : 10 : 0), (b) (90 : 0 : 10), (c) (90 : 9 : 1), (d) (90 : 7 : 3), (e) (90 : 5 : 5), and (f) (90 : 3 : 7).

at room temperature (Fig. 1) indicating the possibility of the respective solid solutions with dissolved LiCl and Na_2WO_4 fractions as well as the slight differences observed in the form of some additional weak diffraction peaks attributable to LiCl with a dissolved sulphate phase and also to the existence of metastable phases. The latter phases are indeed very difficult to discreminate from the XRD patterns. The incorporation of aliovalent (Cl^-) and/or isovalent impurities (WO_4^{2-}) in the host SO_4 ion sublattice affects the host ($LiNaSO_4$) lattice volume which in turn affects the 2θ values, which consequently resulted in slight shifting of diffraction peaks with respect to β-$LiNaSO_4$ (see Figs. 1 and 2). The mixtures are thus considered to be two-phase mixtures of both stable and metastable phases and can be treated as composites.

Since $LiNaSO_4$ (90 mole%) happened to be a bulk matrix in all the studied compositions, the solubility of both WO_4^{2-} and Cl^- was rather limited in the sulfate rich compounds. According to several authors (*45, 46*) the solubility of tungstate is about 5 mole% in the sulfate rich compounds and for Cl^- it is still a question of contradicting ideas (*47, 48*). The phase diagram of Li_2SO_4–LiCl binary system (*47*) shows negligible solid solubility of LiCl in Li_2SO_4 and vice versa. But according to Tilak *et al.* (*48*), the solubility of LiCl in Li_2SO_4 is rather limited (<10 mole%). However, in the present study, it seems likely that $LiNaSO_4$ would possibly dissolve about 3 mole% LiCl. Accordingly, the XRD pattern of $LiNaSO_4$: LiCl (90 : 10 mole%) (Fig. 2a) exhibits two phases; that of $LiNaSO_4$ containing dissolved LiCl as substitutional solid solution and LiCl with a dissolved sulfate phase as second dispersed phase. Thus, the binary mixture of $LiNaSO_4$: LiCl (90 : 10 mole%) is actually an admixture of $(LiNaSO_4)_{ss}$ + $LiCl_{ss}$ and can be regarded as a composite system of two ion conducting matrices.

From Fig. 2b, one can infer $LiNaSO_4$ possibly dissolves 10 mole% Na_2WO_4 and the composition $LiNaSO_4$: Na_2WO_4 (90 : 10) is a solid solution of dissolved WO_4^{2-} into the host SO_4-ion sublattice. Based on the above inferences about the solid solubility limits of LiCl and Na_2WO_4 in $LiNaSO_4$, the $LiNaSO_4$: LiCl : Na_2WO_4 composite mixtures are hence treated as the solid solution of $LiNaSO_4$ with dissolved LiCl as well as Na_2WO_4 along with a chloride phase with dissolved sulfate phase as second dispersed phase and also there might be some metastable phases present. These views have further been strengthened by Raman spectral studies (*49*).

2. *Differential Scanning Calorimetry*

In the present study, besides determining the onset of transition temperatures, DSC has been used to study the phase behavior of the present multicomponent systems such as solid solubility, the formation of two- or multiphase mixtures and associated heat of enthalpies across the solid phase transition.

The typical DSC heat mode traces for the different compositions of $LiNaSO_4$: LiCl : Na_2WO_4 are shown in Figs. 4a–4d. The DSC effects are summarized in Table I. In Figs. 3b and 3c, the traces corresponding to $LiNaSO_4$: LiCl (90 : 10 mole%) and $LiNaSO_4$: Na_2WO_4 (90 : 10 mole%) reciprocal salt systems are shown. From Figs. 3b and 3c four thermal events are evident:

i. An endotherm at 508.75°C with 148 kJ/kg heat of transition previously identified with the β–α transition in $LiNaSO_4$ and the effect of addition of aliovalent impurity (Cl^-) has resulted in the depression of the β–α transition in the host matrix ($LiNaSO_4$). The fact is that the formation of $LiNaSO_4$/LiCl solid solution affects the high conducting phase transition in $LiNaSO_4$ (trigonal → bcc) and consequently T_t drops down to 508.75°C.

ii. An endotherm at 476°C is attributed to a transition reported to occur between the phase boundaries of Li_2SO_4–Li_2Cl_2 in the Li_2SO_4–Na_2SO_4–LiCl reciprocal salt system due to excess undissolved LiCl (*50*).

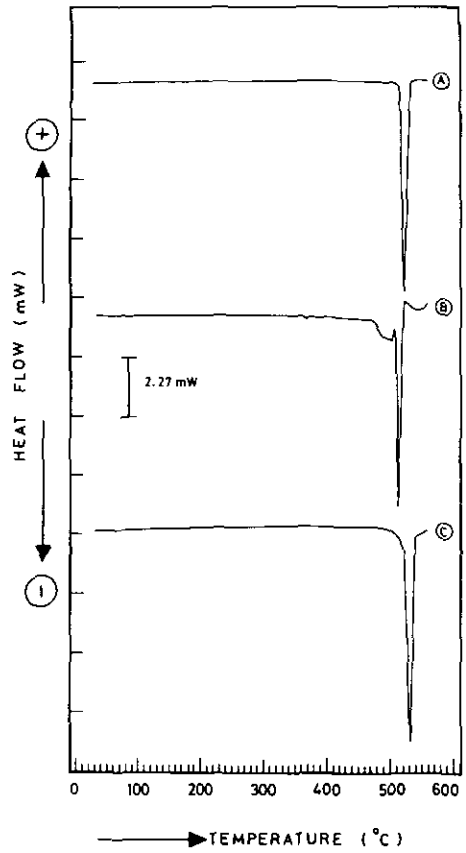

FIG. 3. Differential Scanning Calorimetry (DSC) traces of (A) equimolar-$LiNaSO_4$, (B) $LiNaSO_4$: LiCl (90 : 10 mole%), and (C) $LiNaSO_4$: Na_2WO_4 (90 : 10 mole%).

iii. Two very minor kinks with peak temperatures at 368°C and 392°C were also observed for $LiNaSO_4$: 10 mole% LiCl and which are probably insignificant in view of the fact that no such kinks are reported to occur both in $LiNaSO_4$ and LiCl. These kinks are probably the result of the formation of metastable phases. The cause for the existence of these metastable phases may be explained in the following manner; i.e., the mixture of 90 mole% $LiNaSO_4$ and 10 mole% LiCl corresponds to the composition $Li_{1.05}Na_{0.95}(SO_4)_{0.90}Cl_{0.10}$. If the melt is cooled slowly, the resulting compound would consist of bcc-$Li_{1.05}Na_{0.95}SO_4$ with some dissolved chloride fractions which solidifies at about 600°C and some Li_2SO_4 will be present together with the mixture of chloride phase. But in the present study, instead, the sample was quenched at room temperature. It is likely that a fraction of the lattice defects produced at the high temperatures on melting is retained on rapid cooling and in that case, there might be both stable and metastable phases present and also several phases are probably present only in small quantities.

iv. In $LiNaSO_4$: Na_2WO_4 (90 : 10

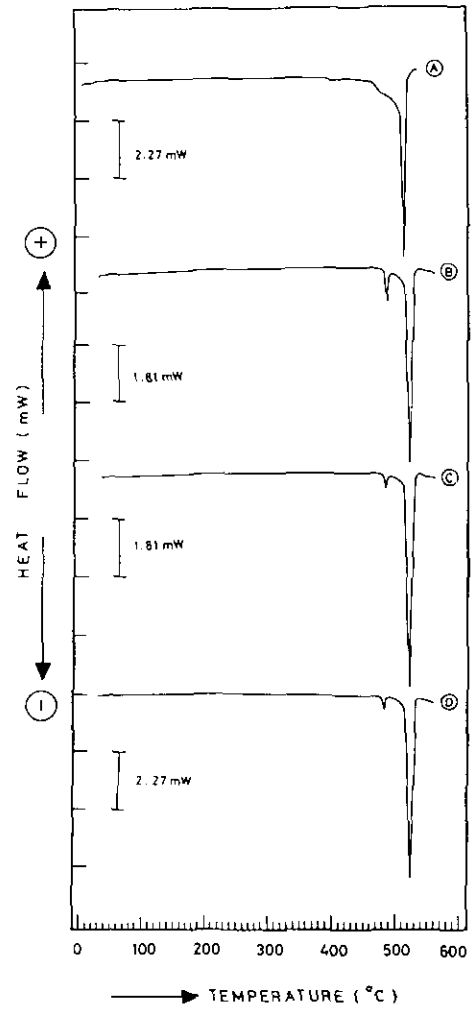

FIG. 4. Differential Scanning Calorimetry (DSC) traces of $LiNaSO_4$: LiCl : Na_2WO_4 mixed systems in the following composition: (A) (90 : 9 : 1), (B) (90 : 7 : 3), (C) (90 : 5 : 5), and (D) (90 : 3 : 7).

TABLE I

SUMMARY OF DSC RESULTS FOR DIFFERENT COMPOSITE MIXTURES OF $LiNaSO_4$: LiCl: Na_2WO_4

Composition (mole%)	Transition temperature T_t/°C				$\Delta H_t^{\rightarrow}$ (kJ/kg)
	I	II	III	IV	
$LiNaSO_4$	≃517[a]				≃130
	518[b]				155
$x LiNaSO_4 : y LiCl : z Na_2WO_4$					
$x:y:z$					
90:10:0	~509	476	368	392	148
90:0:10	~523	—	—	—	152
90:9:1	507	~467	~411	—	147
90:7:3	515	480	—	—	128
90:5:5	~514	477	—	—	137
90:3:7	~515	477	—	—	~133

Note. x, y, and z are mole percentages of the components.

[a] Data from this work.

[b] After Schroeder *et al.* (*14*). $\Delta H_t^{\rightarrow}$ corresponds to transition enthalpy across I transition.

mole%), in Fig. 3c, the transition occurs at 523°C was attributed to the β–α transition in the host matrix ($LiNaSO_4$) and the appearance of this transition shows that Li $NaSO_4$ would possibly dissolve 10 mole% Na_2WO_4 and the reciprocal salt system Li $NaSO_4$: Na_2WO_4 (90:10 mole%) can be treated as solid solution of $LiNaSO_4$ with dissolved Na_2WO_4. The addition of 10 mole% Na_2WO_4 into the host matrix (Li $NaSO_4$) increases the transition temperature ($T_t \simeq 523$°C) with respect to α-$LiNaSO_4$ (see Table I).

As far as the ternary composite mixtures are concerned, four different ternary mole fractions of $LiNaSO_4$: LiCl: Na_2WO_4 were tried and the results are shown separately in Figs. 4a–4d for the sake of clarity. The DSC heat effects are also summarized in Table I and show that the addition of LiCl and Na_2WO_4; i.e., the simultaneous introduction of both alio- and isovalent guest anions into the host matrix ($LiNaSO_4$) has resulted in improved thermal properties. In Fig. 4a, the existence of a very minor endothermic kink at 411°C for 90:9:1 composition was probably due to the presence of a metastable phase. The existence of such metastable phase is a common behavior while the mixtures are quenched from the melt. No such kink was observable in the other three mixtures of composition such as 90:7:3, 90:5:5, and 90:3:7 as shown in Figs. 4b–4d. However, the latent heat of transition enthalpies show significant variations (see Table I).

3. Complex ac Impedance Analysis

Impedance data are presented in the form of imaginary, Z'' (capacitive) against real, Z' (resistive) impedances. The typical impedance plots (imaginary part ($-Z''$) as a function of the real part (Z') for different temperatures are reproduced in Figs. 5 and 6 for 90:9:1 and 90:3:7 compositions respectively. A simple Cole–Cole plot consisting of an arc of circle and of a straight line with an angle $\theta \simeq \pi/2$ with Z'' or Z' axis is usually observed. In fact, the circle center is out of the abcissa and the angle is different from $\pi/2$ ($\theta = \pi/4$). The origin of this non-Debye behavior is not straight forward and

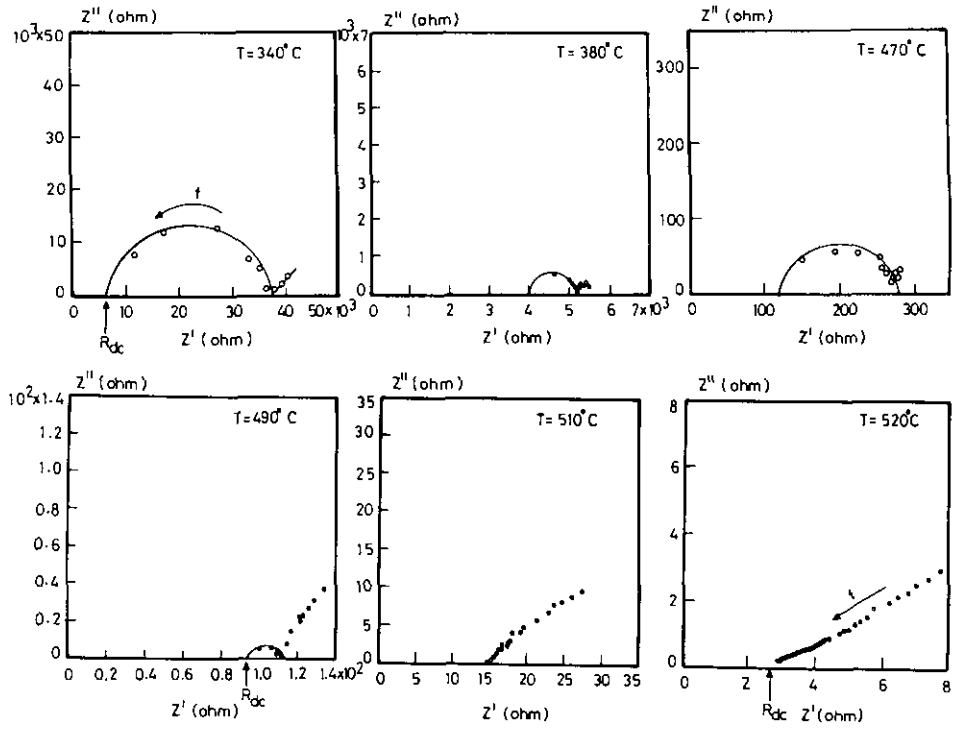

FIG. 5. The typical complex impedance plots for $LiNaSO_4$: LiCl : Na_2WO_4 (90 : 9 : 1) at different temperatures.

various explanations have been proposed in the literature for various materials (*51, 52*). As shown in Figs. 5 and 6, the frequency dispersion of the impedance on the Z' versus Z'' plot gave an undeformed semicircle (or part of the semicircle) and a spike in the low-frequency region.

The impedance data were interpreted by an equivalent circuit which consisted of a parallel RC element with a series capacitance. Conductivity is deduced from the intersect of the arc of the semicircle due to bulk conductivity (σ_{dc}) with Z' axis (real axis). When the temperature rises, the electrode double layer contribution (low-frequency spike) becomes more visible (see Figs. 5 and 6). The collection of various dc conductivity values obtained from the complex impedance plots as a function of temperature were used to draw the Arrhenius plots as shown in Figs. 7 and 8. The log σT versus inverse temperature ($10^3/T$) plot in the present case, can be divided on the basis of different linear regions each associated with different activation energies.

The ionic conductivity (σ) in the solid phase is a composite quantity, basically equal to the triple product of the charge, density, and mobility of the carriers, $\sigma = nq\mu$ where n is the number of charge carriers, q is the charge of carrier and μ is the mobility of the carriers. The increasing trend of conductivity vs inverse temperature ($1/T$) is in accordance with the theory of ionic transport in solids, and usually follows an Arrhenius-type expression,

$$\sigma T = \sigma_0 \exp(-E_a/kT) = (ne^2\lambda^2\nu/kT)\exp(-E_a/kT), \quad (1)$$

where σ_0 represents the composite constant ($ne^2\lambda^2\nu/kT$), which is nothing but the preexponential factor; n, the number of ions per unit volume; e, the ionic charge; λ, the distance between two jump positions; ν, the

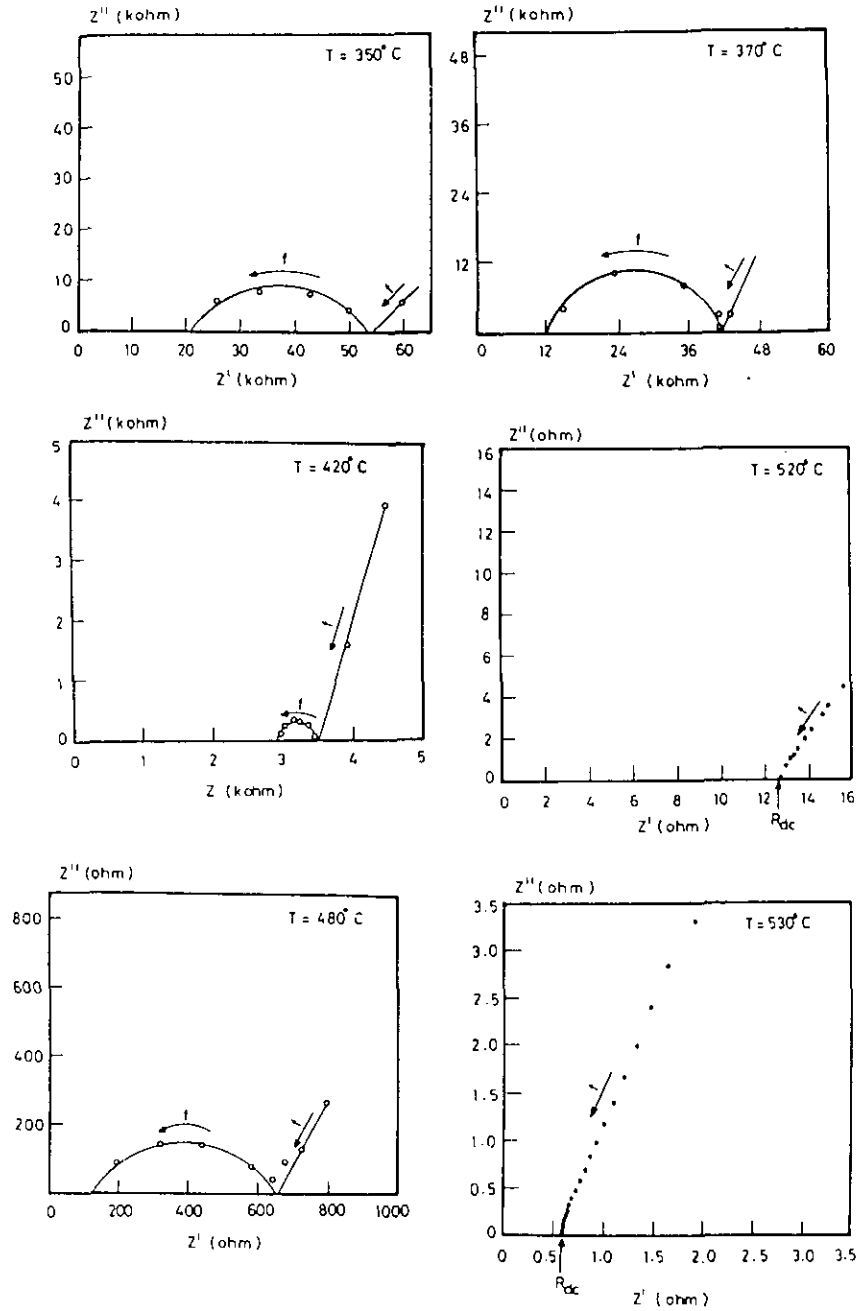

FIG. 6. As in legend to Fig. 5 but for (90 : 3 : 7) composition.

jump frequency; k, the Boltzmann constant; and E_a is the apparent activation energy for ionic motion, assuming the conductivity to be effectively ionic with negligible electronic contribution.

On the basis of Eq. (1), heat mode plots of $\log(\sigma T)$ versus $10^3/T\,(K^{-1})$ are presented in Figs. 7 and 8 for all the compositions studied. Invariably for all the compositions, a slight frequency dependence has been ob-

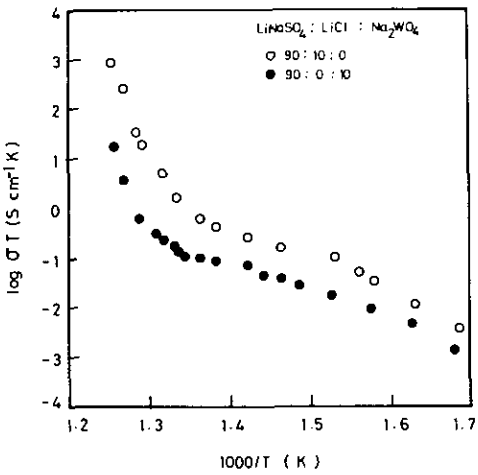

FIG. 7. Plots of log σT versus $10^3/T$ $(K)^{-1}$ of $LiNaSO_4$: LiCl (90 : 10 mole%) (open circles) and $LiNaSO_4$: Na_2WO_4 (90 : 10 mole%) (closed circles) for dc conductivity (extracted from complex impedance plots).

served particularly at lower temperatures as expected where the effects of grain boundary conduction are dominant. The results of conductivity versus composition data are summarized in Table II at two different frequencies along with the dc conductivity values extracted from the complex impedance plane analysis as discussed below.

In view of the frequency dependence of the conductivity at low temperatures, it becomes imperative to determine the dc conductivity at different temperatures for all the composites from the measured ac impedance data (Z' and Z'').

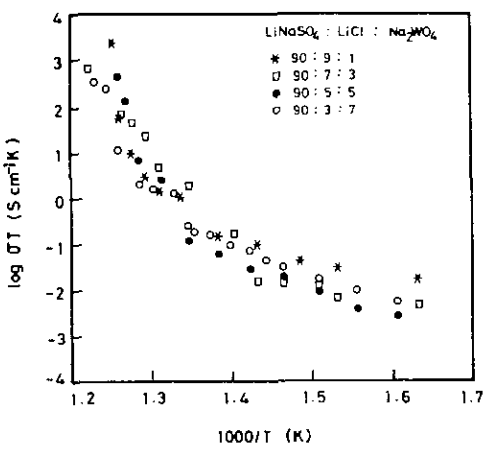

FIG. 8. Plots of log σT versus $10^3/T$ $(K)^{-1}$ for $LiNaSO_4$: LiCl : Na_2WO_4 at different compositions (in mole%).

The typical impedance plots (Z' vs Z'') at various temperatures are reproduced in Figs. 5 and 6 for the two compositions (90 : 9 : 1 and 90 : 3 : 7, respectively) studied. The complex impedance plots for all the samples were usually semicircular with a tail at the low-frequency side in the somewhat low-temperature region. The equivalent circuit may consist of a simple resistance–capacitance parallel combination with an additional capacitor connected in series. As temperature increases the low frequency residual tail becomes more visible due to increasing value of sample–electrode double layer capacitance (C_{dl}).

This effect is clearly seen invariably at high temperatures for all the compositions studied. In the complex impedance representation, as shown Figs. 5 and 6, the low-frequency response appears as an inclined spike and such a spike (tail-like) is characteristic of a blocking double-layer capacitance, whose magnitude may be estimated from any position on the spike using the equation $Z'' = \frac{1}{2}\pi fC$ where f, the frequency and C, the capacitance associated with the frequency f. Values of about $2\mu f$ are obtained which are typical of those expected for the blocking of ionic charge carriers at the metal–sample interface (*53*). The disappearance of the semicircular portion in the complex impedance plots as temperature increases invariably for all the samples and the increasing response of the low-frequency spike led to a conclusion that the current carriers are ions and this leads one to further conclude that the total conductivity is mainly the result of ion conduction.

In the present study, the main interest was focused only towards the electrical and thermal properties of the mixtures comprising $LiNaSO_4$, LiCl and Na_2WO_4. The two binary salt systems $LiNaSO_4$: LiCl (90 : 10 mole%) and $LiNaSO_4$: Na_2WO_4 (90 : 10 mole%) have also been tried as starting

TABLE II

THE ELECTRICAL CONDUCTIVITY OF $x LiNaSO_4 : y LiCl : z Na_2WO_4$ COMPOSITES AT DIFFERENT FREQUENCIES

Composition (mole%)	Temp. (°C)	$\sigma_{1\,kHz}$ (S/cm)	$\sigma_{10\,kHz}$ (S/cm)	σ_{dc} (S/cm)
90 : 10 : 0[a]	340	9.5×10^{-6}	1.0×10^{-5}	2.0×10^{-5}
	360	4.7×10^{-5}	5.0×10^{-5}	6.0×10^{-5}
	470	1.3×10^{-3}	1.2×10^{-3}	1.3×10^{-3}
	500	2.5×10^{-2}	2.4×10^{-2}	2.5×10^{-2}
	505	4.3×10^{-2}	4.4×10^{-2}	4.5×10^{-2}
	525	6.1×10^{-1}	6.7×10^{-1}	1.1×10^{0}
90 : 0 : 10[b]	342	5.7×10^{-6}	6.8×10^{-6}	8.0×10^{-6}
	362	1.14×10^{-5}	1.2×10^{-5}	1.5×10^{-5}
	470	1.42×10^{-4}	1.5×10^{-4}	1.5×10^{-4}
	503	8.3×10^{-4}	8.5×10^{-4}	8.4×10^{-4}
	523	2.1×10^{-2}	2.2×10^{-2}	2.3×10^{-2}
90 : 9 : 1	340	4.0×10^{-6}	5.4×10^{-6}	3.1×10^{-5}
	380	3.1×10^{-5}	3.7×10^{-5}	5.0×10^{-5}
	475	5.7×10^{-4}	5.8×10^{-4}	1.6×10^{-3}
	500	4.0×10^{-3}	4.0×10^{-3}	4.0×10^{-3}
	524	1.5×10^{0}	2.1×10^{0}	3.0×10^{0}
90 : 7 : 3	340	1.3×10^{-6}	2.0×10^{-6}	7.5×10^{-6}
	380	3.8×10^{-6}	2.5×10^{-6}	1.0×10^{-5}
	470	2.5×10^{-3}	2.5×10^{-3}	2.6×10^{-3}
	500	2.6×10^{-2}	2.9×10^{-2}	3.0×10^{-2}
	520	1.3×10^{-1}	2.1×10^{-1}	1.5×10^{-1}
90 : 5 : 5	350	3.9×10^{-6}	4.1×10^{-6}	4.4×10^{-6}
	370	5.8×10^{-6}	5.6×10^{-6}	6.3×10^{-6}
	470	1.5×10^{-4}	1.5×10^{-4}	1.6×10^{-4}
	505	9.0×10^{-3}	9.0×10^{-3}	9.1×10^{-3}
	515	1.7×10^{-1}	1.7×10^{-1}	1.8×10^{-1}
	521	5.7×10^{-1}	5.6×10^{-1}	6.0×10^{-1}
90 : 3 : 7	350	6.6×10^{-6}	4.5×10^{-6}	9.2×10^{-6}
	370	6.6×10^{-6}	1.2×10^{-5}	1.6×10^{-5}
	442	1.2×10^{-4}	1.3×10^{-4}	1.4×10^{-4}
	470	2.7×10^{-4}	3.3×10^{-4}	3.5×10^{-4}
	505	9.4×10^{-4}	1.2×10^{-3}	2.7×10^{-3}
	520	1.3×10^{-2}	1.4×10^{-2}	1.5×10^{-2}

Note. σ_{dc} refers to dc conductivity obtained from complex impedance analysis (see text) (x, y, and z are mole percentages of the respective components)

[a] Reciprocal salt system of composition, $Li_{1.05}Na_{0.95}(SO_4)_{0.90}Cl_{0.10}$.

[b] Reciprocal salt system of composition, $Li_{0.9}Na_{1.1}(SO_4)_{0.90}(WO_4)_{0.10}$.

points before the mixtures of $LiNaSO_4$–$LiCl$–Na_2WO_4 were tried.

3.1 $LiNaSO_4 : LiCl$ composites. The dc electrical (ionic) conductivity of $LiNaSO_4$: LiCl (90 : 10 mole%) shows an increasing trend in the direction of increasing temperature. The variation of electrical conductivity (log σT) versus inverse of temperature for $LiNaSO_4$: LiCl (90 : 10 mole%) is shown in Fig. 7a (marked as ○).

$LiNaSO_4$: LiCl (90 : 10 mole%) reciprocal salt system of composition $Li_{1.05}Na_{0.95}$

$(SO_4)_{0.90}Cl_{0.10}$ was examined for the first time in an effort to find a new Li^+-based solid electrolyte. In the present case, LiCl was chosen as an additive because the Cl^- ions will act as an aliovalent[1] impurity for the host SO_4 ions, and also because LiCl is one of the renowned lithium salts which does not pose great problems regarding handling etc., despite its hydroscopic nature. The solubility of LiCl in Li_2SO_4 based materials is very small, even less than 10 mole%. Of course, the phase diagram of Li_2SO_4–LiCl binary system (*47*) shows negligible solubility on either side. Therefore, it is clear that no definite report is available on LiCl solubility in alkali sulfate rich compounds in the literature. Nevertheless, from the present study, it has been confirmed from XRD and DSC (see the details elsewhere in this paper) measurements that $LiNaSO_4$ can dissolve about 3 mole% LiCl. The detailed phase diagram of the Li_2SO_4–Na_2SO_4–LiCl reciprocal salt system as part of the $Li^+, Na^+//Cl^-, SO_4^{2-}$ quaternary reciprocal system is known (*50*).

In order to discuss the conductivity behavior of the $LiNaSO_4$–LiCl composite, two different composition regions are encountered: (i) in which the two salt systems form solid solution and (ii) a two-phase mixture. The above two areas, i.e., fast-ion transport in mixed crystals or solid solutions and two- or multiphase mixtures have only recently emerged as areas of considerable interest. The latter may be named as an aluminaless composite solid electrolytes (*54*). It is well known that the dispersion of fine insulating particles of Al_2O_3 in a solid electrolyte matrix enhances the ionic conductivity (*55*). The phenomenon was first thought to be due to something unique. However, the studies on AgI–AgBr, AgI–fly ash, AgI–SiO_2 (*56–58*), and recently on Li_2SO_4–LiCl (*48*), β-Li_2SO_4–Na_2SO_4 (*54*), $Li_2Mg_2(SO_4)_3$ + Na_2SO_4 (*59*), Li_2WO_4–Li_2SO_4 (*60*), Li_2SO_4–Li_2CO_3 (*61*), Li_2SO_4–$CaSO_4$, Li_2SO_4–$MgSO_4$ (*62*), etc., dispelled these ideas and pointed out the fact that the enhanced electrical transport in multiphase mixtures was a rather general phenomenon and not merely limited to fine Al_2O_3 particles.

The experimental activities in these areas have been backed by theoretical models proposed to explain the enhanced electrical transport in the solid solutions as well as in multiphase mixtures (*63–68*). It has also been shown that the electrical transport of some two-phase systems can be described by using effective medium percolation theory (*69–71*).

The effect of addition of a finite quantity (10 mole%) of LiCl into $LiNaSO_4$ bulk matrix resulted in higher conductivities when compared to pure equimolar-$LiNaSO_4$ at specific temperatures and the values are highlighted in Table II. The highest conductivity achieved in the present reciprocal system is about 37 times larger (σ_{dc} = 5.6×10^{-5} S/cm at 360°C) than that of β-$LiNaSO_4$ (σ_{dc} = 1.5×10^{-6} S/cm) (*36*) and ~15 times larger at 500°C. At 525°C, the σ_{dc} value of $LiNaSO_4$: LiCl (90 : 10 mole %) increases to 1.1 S/cm, which is fairly high when compared to 0.8 S/cm at 526.8°C for α-$LiNaSO_4$ (*13*).

In the $\log(\sigma T)$ versus $10^3/T$ plot (Fig. 7), there is a slight upward curved deviation from the straight line with a sigmoidal character in the high-temperature region of the plots as has been observed for many other solid solutions as well as two-phase mixtures. This curvature may be due to a temperature dependence of the formation and migration enthalpies of aliovalent impurities (Cl^-). The increase in the conductivity of $LiNaSO_4$: LiCl (90 : 10 mole%) system is attributed to the substitution of Cl ions for SO_4 ions; i.e., due to the formation of solid solution by the incorporation of ion (Cl^-) vacancies and thus the addition of each Cl^- would generate a cation vacancy and also suppress the concentration of cation interstitials because of the mass action law (*72*).

[1] It has recently been suggested that to determine the migration enthalpies for vacancies and interstitials in $LiNaSO_4$ crystals, controlled doping with aliovalent impurities should be performed (*35*).

The increase in conductivity, nevertheless, in the present case, cannot only be explained by the theory of classical doping but, since the results are very much comparable with those of dispersed second phase solid electrolyte systems, they can be explained on the basis of dispersed phase theory (*66*). The dispersed second phase due to grains of LiCl containing dissolved sulfate phase can provide large interfacial or overlap region for ion conduction. The mechanism of σ enhancement in the present case, seems to be similar to that in γ-Al_2O_3 dispersed solid electrolytes (see more explanations later). The conductivity–composition results as a function of temperature are summarized in Table II.

As for the activation energies, two different linear regions are identified in the plots of $\log(\sigma T)$ versus $10^3/T$. If the two linear regions are labeled as I and II from low temperature to high respectively, region I is associated with an activation energy, E_a = 0.60 eV in the range 320–460°C, may be identified as the extrinsic-conduction region (or extrinsic dissociated region) in which all carrier ions or defects are free and the enthalpy of activation (E_a = 0.60 eV) is just related to migration enthalpy of vacancies (h_m^v) or interstitials (h_m^i). Therefore

$$E_a(I)\,(\text{extrinsic}) = h_m^i \text{ or } h_m^v = 0.60\,\text{eV}. \quad (2)$$

The high-temperature region II from 460–505°C is the intrinsic region of conduction. Assuming Frenkel disorder, the conductivity in the intrinsic temperature range, where the ionic conductivity is determined by thermally activated crystal defects, can be described by

$$\sigma T = \sigma_0 \exp\left[-\frac{h_f/2 + h_m}{kT}\right]. \quad (3)$$

A knee point at 460°C separates both the regions (where σ attains a value of 8.7×10^{-4} S/cm) at which a linear upward departure has been noticed with change of slope in the linear portion associated with a different activation energy E_a = 2.46 eV. Therefore, one can write,

$$E_a(\text{II})\,(\text{intrinsic}) = h_f/2 + h_m^i \text{ or } h_m^v = 2.46\,\text{eV}. \quad (4)$$

From Eq. 3 and 4, we get,

$$h_f = 2\{E_a(\text{II}) - h_m^i \text{ or } h_m^v\}$$
$$h_f = 3.7\,\text{eV}. \quad (5)$$

And further, σ values increase markedly beyond the phase transition temperature (~509°C), and attains a value of 1.1 S/cm which is somewhat high compared to pure equimolar-$LiNaSO_4$ (σ = 0.8 S/cm at 526.8°C) (*13*) (However, our reinvestigation results on $LiNaSO_4$ show that σ has the value of only 0.62 S/cm at 530°C). The enhanced σ values in the present case [$LiNaSO_4$: LiCl (90 : 10 mole%)] are due to the presence of two solid phases and perhaps both the phases are possessing high conductivities at high temperatures. However, the enhancement in the conductivity is primarily a result of the increase in concentration of the charge carriers (ions or vacancies) forming a well-defined diffuse space-charge layers and thus the overall defect concentration in the space-charge region may be one of the key parameters for the high conduction. Hence, the total conductivity of the biphasic matrix ($(LiNaSO_4)_{ss}$ and $(LiCl)_{ss}$), including the contribution from the space-charge region in the present case may be written as

$$\sigma_{\text{total}} = \sigma_b + \sigma_{b'} + \sigma_s \quad (6)$$

where σ_b and $\sigma_{b'}$ are the bulk conductivities of $(LiNaSO_4)_{ss}$ and $(LiCl)_{ss}$ respectively, and σ_s is the space-charge contribution.

3.2 $LiNaSO_4$: Na_2WO_4. $LiNaSO_4$: Na_2WO_4 (90 : 10 mole%) mixed binary alkali anion system was examined in an effort to find the effect of incorporation of larger-radius guest WO_4 ion into $LiNaSO_4$ host matrix.

A small amount (10 mole%) of Na_2WO_4 was added instead of LiCl into $LiNaSO_4$ bulk matrix to examine the influence of larger radius guest anion (WO_4) into smaller radius host sulfate anion sublattice in the

TABLE III

THE EXTRINSIC AND INTRINSIC ACTIVATION ENERGIES (E_a^I AND E_a^{II}, RESPECTIVELY) CALCULATED FROM THE dc ARRHENIUS PLOT OF xLiNaSO$_4$:yLiCl:zNa$_2$WO$_4$ COMPOSITE SYSTEMS

Composition (mole%)	E_a (eV)	Temp. range (°C)
90:10:0[a]	E_a^I = 0.60 eV	320–460
	E_a^{II} = 2.46 eV	460–505
90:0:10[b]	E_a^I = 0.47 eV	322–470
	E_a^{II} = 2.53 eV	470–523
90:9:1	E_a^I = 0.33 eV	340–450
	E_a^{II} = 1.89 eV	450–524
90:7:3	E_a^I = 0.24 eV	340–425
	E_a^{II} = 1.80 eV	425–545
90:5:5	E_a^I = 0.55 eV	350–470
	E_a^{II} = 3.38 eV	470–521
90:3:7	E_a^I = 0.55 eV	350–470
	E_a^{II} = 3.15 eV	495–540

Note. x, y, and z are mole percentages of the respective components.

[a] Reciprocal salt system of composition, $Li_{1.05}Na_{0.95}(SO_4)_{0.90}Cl_{0.10}$.

[b] Reciprocal salt system of composition, $Li_{0.9}Na_{1.1}(SO_4)_{0.90}(WO_4)_{0.10}$.

present case. The $\log(\sigma T)$ versus $10^3/T$ plot for dc conductivity data obtained from the complex impedance plane analysis for Li NaSO$_4$:Na$_2$WO$_4$ (90:10 mole%) is shown in Fig. 7 (marked as ●). The conductivity and activation energy (E_a) for ion conduction are summarized in Tables II and III, respectively. The conductivity of LiNaSO$_4$:Na$_2$WO$_4$ (90:10 mole%) is about 10 times higher at 362°C (σ_{dc} = 1.52 × 10^{-5} S/cm) than the values of 1.7 × 10^{-6} S/cm at 360°C for β-LiNaSO$_4$ (*54*) and also from the value (1.81 × 10^{-6} S/cm at the same temperature) of our reinvestigation results on LiNaSO$_4$ system (*36*). The enhanced cationic conductivity by a factor of 10 in the extrinsic region of conduction is attributed to the presence of larger radius guest WO$_4$ ion into LiNaSO$_4$ host matrix which tends to open up more space for the mobile cations (Li^+ and Na^+) to move freely through the host lattice framework and which suggests the dominant role of simple lattice expansion in facilitating the cationic mobility in this reciprocal salt system of composition $Li_{0.9}Na_{1.1}(SO_4)_{0.9}(WO_4)_{0.1}$.

In the high temperature region of conduction at or near the transition, the conductivity starts decreasing. That is, at 503°C, the σ_{dc} attains a value of only 8.4 × 10^{-4} S/cm which is low when compared to β-LiNaSO$_4$ (σ = 1 × 10^{-3} S/cm) at 500°C. And at 523°C (T_t), the σ value is only 2.3 × 10^{-2} S/cm which is about 10 times less than that of equimolar-LiNaSO$_4$ at 526.8°C (σ = 0.8 S/cm) (*13*). It should be mentioned here that the σ values at or near the solid-phase transition are low for the present reciprocal mixture containing 10 mole% Na$_2$WO$_4$ and the cause is that the presence of isovalent larger radius guest WO$_4$ ion would lower the conductivity.

The decrease in σ near the transition could be explained in the following manner; i.e., the introduction of larger radius isovalent tetrahedral WO$_4$ anion in the regular lattice sites of smaller SO$_4$ anion in the host lattice network (LiNaSO$_4$) tends to increase the lattice density which significantly affects the rotational freedom of tetrahedral SO$_4$ anion in the host matrix as evident from the increase in activation energy (see below) for migration resulting in the observed drop in conductivity.

In the present case, the obtained activation energy, E_a = 0.47 eV, in the temperature range between 322 and 470°C and the high-temperature region associated with a higher activation energy of 2.53 eV between 470 and 523°C. (However, Secco (*73*) has given the value of activation energy obtained from his own measurements for Li NaSO$_4$:Na$_2$WO$_4$ (90:10 mole%) as 0.30 ± 0.2 eV, without mentioning the temperature range.)

The findings in the particular case are that the addition of 10 mole% Na$_2$WO$_4$ significantly affects the cubic transition in Li NaSO$_4$ and shifts the solid-phase transition (T_t) to 523 from 518°C. In the low temperature extrinsic region of conduction, the values are slightly higher in $Li_{0.9}Na_{1.1}$

$(SO_4)_{0.9}(WO_4)_{0.1}$ reciprocal system than the pure equimolar $LiNaSO_4$ and this is attributed to simple host lattice volume expansion by incorporating larger radius isovalent guest WO_4 ion into its respective sublattice facilitating the freedom of cation movement due to the large number of accessible interconnected sites resulting in enhanced conductivity. In contrast, at or near the high-temperature phase formation, the conductivity decreases considerably even about 10 times, and the cause is perhaps the result of the increase in host lattice density due to the presence of larger radius isovalent guest anion (WO_4), which tends to obstruct the rotation/reorientational motion of SO_4 ion in the host lattice.

3.3 $LiNaSO_4$: LiCl : Na_2WO_4 composites. The results of electrical conductivity of Li $NaSO_4$: LiCl : Na_2WO_4 composites are also given in Table II. The $\log(\sigma T)$ versus $10^3/T$ plots are presented in Fig. 8. From Table II, it is inferred that the results of conductivity change with increasing Na_2WO_4 content (in mole%) or in other words, σ value drops while decreasing the LiCl content. Among the four compositions (90 : 9 : 1, 90 : 7 : 3, 90 : 5 : 5, and 90 : 3 : 7) studied, the most successful composition was found to be LiNa SO_4 : LiCl : Na_2WO_4 (90 : 9 : 1), which has a solid phase transition at 507°C with the heat of transition enthalpy 147 kJ/kg. This particular transition may be correlated to the solid-phase transition in equimolar-$LiNaSO_4$ (β–α) at 518°C with the latent heat of transition of 155 kJ/kg. Besides, two other transitions occur at 469 and 411°C. The one at 469°C could be attributed to the presence of LiCl phase. However, it should be pointed out the fact that the transition occurs at 469°C was not detectable in the σ measurements and hence the value determined by DSC has to be relied upon. The σ value is slightly higher ($\sigma_{dc} = 4 \times 10^{-3}$ S/cm) than that of equimolar-$LiNaSO_4$ at 500°C ($\sigma_{dc} = 1 \times 10^{-3}$ S/cm). But after the phase transition (T_t = 507°C), the σ_{dc} increases drastically and attains a value of 3.0 S/cm. The existence of extremely high conductivity at 520°C for $LiNaSO_4$: LiCl : Na_2WO_4 (90 : 9 : 1) composition, after referring to the corresponding DSC thermogram (Fig. 4) reveals that the higher conductivity is due to the presence of two solid phases and perhaps there is a reason to conclude that both the phases are possessing high conductivities. And moreover, no evidence of disk deformation or dimensional changes was observed in the cooled pellet after the conductivity experiments. This particular observation conclusively proves that the very high conductivity is not due to the presence of a solid–liquid multiphase. Below the transition (T_t = 507°C), the σ enhancement may be attributed to the increase in interfacial conductivity due to the grains of dispersed phase (LiCl with a dissolved sulfate phase) by the composite effect. There has been several models developed in the area of the so-called composite solid electrolyte systems so far (*66, 67, 74*). Among the following models (a) polycrystalline materials (*MX/MX*) (*66*), (b) conducting–conducting (*MX/MX'*) (*67*), are of interest as far as the present study is concerned. The present conductivity results can very well be reconciled to the above two models and a plausible explanation for the conductivity enhancement based on the above two models is as follows; since the observed conductivity is much higher than each of the individual phases present therein, an enhancement in the conductivity is primarily due to the increase in concentration of the charge carriers (ions or vacancies) forming a diffuse space-charge layer (*75*). The formation of a space-charge layer at different interfaces is as follows: (a) at the interface of $(LiCl)_{ss}$ and $(LiNaSO_4$–LiCl–$Na_2WO_4)_{ss}$, it is similar to that as in the case of *MX/MX* (*66*), and (b) at the interface between two ionically conducting phases it is equivalent to that of *MX/MX'* (*67*).

At the interface of two ion conductors (*MX/MX'*), the transport of the ions is not only parallel to the interface, but an additional contribution comes from an interface into the other conductor; i.e., net transfer

of ions from MX to MX' is also favorable (*76*). Therefore, in the present case, the conductivity across the grain boundaries is also of equal importance.

As far as other compositions (90 : 7 : 3, 90 : 5 : 5, and 90 : 3 : 7) are concerned, while varying both LiCl and Na_2WO_4 contents simultaneously gave less favorable results compared to 90 : 9 : 1 composition, i.e., the transition temperatures show increasing trend, but in the same time, latent heat of transitions indicate the decreasing trend as seen in Table III. It should be mentioned here that the values at or above solid-phase transition is comparatively low for the three ternary mixtures, viz., 90 : 7 : 3, 90 : 5 : 5, and 90 : 3 : 7. The decreasing trend in σ values for these compositions suggests that the increasing addition of Na_2WO_4 content would lead to lower the conductivity and that the incorporation of Cl and WO_4 ions in the regular host lattice sites of SO_4 ion simultaneously, is equivalent to an increase in lattice density or a decrease in free volume in the host volume network resulting in the observed drop in conductivity (*77, 78*).

Conclusions

The six systems that have been investigated can be categorized in three ways based on the nature of the additives used. The first category includes the system where the dopant is an aliovalent ion, i.e., $LiNaSO_4$–LiCl system. The monovalent Cl^- ions act as aliovalent impurity for $LiNaSO_4$, because the host anion (SO_4) is divalent. The second one includes a system in which the dopant is isovalent; i.e., the constitutent ions of the dopant have the same valency as the host ion ($LiNaSO_4$–Na_2WO_4). The third category includes both alio- and isovalent dopants simultaneously into the host matrix, i.e., $x LiNaSO_4$–y LiCl–z Na_2WO_4, where x, y, z are the mole fractions of the respective salts.

As far as $LiNaSO_4$: LiCl (90 : 10 mole%) binary mixture is concerned, it is found that $LiNaSO_4$ possibly dissolves about 3 mole% LiCl and the excess LiCl content forms a second dispersed phase, and which are indicated by XRD patterns. The high temperature solid-phase transition (β–α) in $LiNaSO_4$ in the present case is still present even when it contains small amount of LiCl and the transition temperature drops down to ~509 from 518°C and which are confirmed by DSC effects. The enhanced electrical conductivity is attributed not only to the introduction of defects due to aliovalent guest (Cl^-) ion substitution, but also due to grains of dispersed phase (excess LiCl) by the composite effect. This study also suggests that the enhancement in σ is not merely limited to just dispersion of Al_2O_3, but is a more general phenomenon.

For $LiNaSO_4$: Na_2WO_4 (90 : 10 mole%) system, even though the solid solubility of WO_4 ion into SO_4 sublattice is rather limited, our XRD indicates the possibility of solid solution of $LiNaSO_4$ with dissolved Na_2WO_4 (10 mole%). The addition of 10 mole%) Na_2WO_4 significantly affects the cubic transition (T_t) and shifts to 523 from 518°C. As far as the conductivity results are concerned, the addition of Na_2WO_4 gave less favorable results; i.e., at or near the high-temperature phase formation the σ decreases by about 10 times and the cause is perhaps due to increase in lattice density which obstructs the freedom of cation migration inside the host lattice.

As far as ternary composite mixtures are concerned, the most successful composition was found to be $LiNaSO_4$: LiCl : Na_2WO_4 (90 : 9 : 1), which has a transition at 507°C with the transition enthalpy of 147 kJ/kg. Of course, the addition of both LiCl and Na_2WO_4 simultaneously into $LiNaSO_4$ matrix gave favorable results, but diminishes the heat of transition enthalpy. The evolution of conductivity with temperature gave better improvement for the chosen composition of 90 : 9 : 1 with respect to pure equimolar-$LiNaSO_4$. Whereas, the other compositions viz., 90 : 7 : 3, 90 : 5 : 5, and 90 : 3 : 7 gave less favorable results; of course, these three compositions offer the choice of lower

transition temperature, but these are accompanied by lower transition enthalpies.

Acknowledgments

Authors wish to express their thanks to Professor S. K. Rangarajan, Director, CECRI, India for the kind permission to carry out the impedance analysis. One of us (SRSP) is grateful to Professor T. M. Haridasan for the keen interest and encouragement toward this research work. We would like to express our thanks to the referees for their useful suggestions to improve the presentation. Our special thanks to Dr. S. V. K. Iyer, Dr. N. Anbananthan, and Dr. H. P. Sharma, CECRI, India, for their help in various stages of this work.

References

1. G. D. Mahan and W. L. Roth (Eds.), "Superionic Conductors," Plenum, New York (1976).
2. S. Geller (Ed.), "Solid Electrolytes," Springer-Verlag, Berlin (1977).
3. P. Hagenmuller and W. Van Gool (Eds.), "Solid Electrolytes, General Principles, Characterization, Materials and Application," Academic Press, New York (1978).
4. P. Vashishta, J. N. Mundy, and G. K. Shenoy (Eds.), "Fast Ion Transport in Solids," North-Holland, New York (1979).
5. J. W. Perram and S. de Leeuw (Eds.), "Physics of Superionic Conductors and Electrode Materials," Proc. NATO ASI, Denmark (1980).
6. C. Julien, *Mater. Sci. Eng. B* **6,** 9 (1990).
7. R. G. Linford, *Solid State Ionics* **28–30,** 331 (1988).
8. F. Beniere, *La Recherche* **52,** 36 (1975).
9. S. Chandra (Ed.), "Superionic Solids," North-Holland, Amsterdam (1981).
10. A. L. Laskar and S. Chandra (Eds.), "Materials Science and Technology" series, Academic Press, New York (1989).
11. A. Kvist and A. Lundén, *Z. Naturforsch. A* **20,** 235 (1965).
12. A. Kvist, Ph.D. thesis, Univ. of Gothenburg, Sweden (1967).
13. A. M. Josefson and A. Kvist, *Z. Naturforsch. A* **24,** 466 (1969).
14. K. Schroeder, A. Kvist, and H. Ljungmark, *Z. Naturforsch. A* **27,** 1252 (1972).
15. R. Aronsson, B. Heed, B. Jansson, A. Lundén, L. Nilsson, K. Schroeder, C. A. Sjoblom, J. O. Thomas, and B. C. Tofield, *in* "Fast Ion Transport in Solids" (P. Vashista, J. N. Mundy, and G. K. Shenoy, Eds.) pp. 471–474, North-Holland, Amsterdam (1979).
16. K. Shahi, J. B. Wagner, and B. B. Owens, *in* "Lithium Batteries" (J. P. Gabano, Ed.), pp. 407–448, Academic Press, New York (1983).
17. L. I. Staffansson, *Acta Chem. Scand.* **26,** 2150 (1972).
18. K. Schroeder, Ph.D. thesis, Univ. of Gothenburg, Sweden (1975).
19. B. Morison and D. L. Smith, *Acta Crystallogr.* **22,** 906 (1967).
20. S. Vilminot, L. Cot, and M. Maurin, *Rev. chim. Miner.* 13, 157 (1976).
21. Y. C. Venudhar, L. Iyengar, and K. V. K. Rao, *J. Mater. Sci. Lett.* **4,** 1010 (1985).
22. L. F. Polishchuk and A. K. Bogdanova, *Russ. J. Phys. Chem.* **51,** 1195 (1977).
23. J. N. Sherwood (Ed.), "The Plastically Crystalline State," Wiley, New York (1979).
24. T. Förland and J. Krogh-Moe, *Acta Crystallogr.* **11,** 224 (1958).
25. Arnold Lundén and Leif Nilsson, *J. Mater. Sci. Lett.* **5,** 645 (1986).
26. K.-D. Junke, M. Mali, J. Roos, and D. Brinkmann, *Solid State Ionics* **28–30,** 1329 (1988).
27. J. M. Newsam, A. K. Cheetham, and B. C. Tofield, Ref. (*14*), p. 435.
28. D. Massiot, C. Bessada, P. Echegut, J. P. Coutures, and F. Taulelle, *Solid State Ionics* **37,** 223 (1990).
29. L. Nilsson, N. H. Anderson, and A. Lundén, *Solid State Ionics* **34,** 111 (1989).
30. R. Kaber, L. Nilsson, N. H. Andersen, A. Lundén, and J. O. Thomas, *J. Phys. Condens. Matter,* **4,** 1925 (1992).
31. A. Kvist, A. Bengtzelius, and A. Schiraldi, *in* "Diffusion Processes" (J. N. Sherwood, A. V. Chadwick, W. M. Muir, and F. L. Swinton, Eds.), p. 523, Gordon and Breach, London (1971).
32. A. F. Polishchuk and T. M. Shurzhal, *Sov. Electrochem.* **9,** 902 (1973).
33. K. Singh and V. K. Despande, *Solid State Ionics* **13,** 157 (1984).
34. U. M. Gundusharma, C. Maclean, and E. A. Secco, *Solid State Commun.* **57,** 479 (1986).
35. B.-E. Mellander, B. Graneli, and J. Roos, *Solid State Ionics* **40/41,** 162 (1990).
36. S. R. Sahaya Prabaharan and P. Muthusubramanian, submitted for publication.
37. A. Lundén, *Solid State Ionics* **28/30,** 163 (1988).
38. E. A. Secco, *J. Solid State Chem.* **96,** 366 (1992).
39. M. A. Pimenta, P. Echegut, G. Hauret, and F. Gervais, *Phase Trans.* **9,** 185 (1987).
40. D. Teeters and R. Frech, *Solid State Ionics* **5,** 437 (1981).
41. D. Teeters and R. Frech, *J. Chem. Phys.* **76,** 799 (1982).
42. D. Teeters and R. Frech, *Solid State Ionics* **5,** 437 (1984).
43. L. Borjesson and L. M. Torrell, in "Proc. Electro. Chem. Soc., Meeting," Las Vegas (1985).

44. S. R. SAHAYA PRABAHARAN, P. MUTHUSUBRAMANIAN, AND L. MATHIVANAN, *in* "Proc. Solid State Ionics Materials and Applications" (B. V. R. Chowdari, S. Chandra, Shri Singh and P. C. Srivastava, Eds.), p. 415, World Scientific, Singapore (1992).

45. G. PRAKASH AND K. SHAHI, *Solid State Ionics* **23,** 151 (1987).

46. R. P. GUNAWARDANE, M. A. K. L. DISSANAYAKE, AND F. P. GLASSER, *Br. Ceram. Trans. J.* **88,** 45 (1989).

47. A. LUNDÉN, B. E. MELLANDER, A. BENGTZELIUS, H. LJUNGMARK, AND R. TARNEBERG, *Solid State Ionics* **18–19,** 514 (1986).

48. A. V. N. TILAK, M. UMAR, AND K. SHAHI, *Solid State Ionics* **24,** 121 (1987).

49. S. R. SAHAYA PRABAHARAN, Ph.D. Thesis, Madurai Kamaraj Univ., India (1992).

50. E. K. AKOPOV AND A. G. BERGMAN, *Dokl. Akad. Nauk SSSR* **102,** 82 (1955).

51. K. S. COLE AND R. H. COLE, *J. Chem. Phys.* **2,** 341 (1941).

52. P. DEBYE, "Polar Molecules," Dover, New York (1945).

53. J. T. S. IRVINE, D. C. SINCLAIR, AND A. R. WEST, *Adv. Mater.* **3,** 132 (1990).

54. S. CHAKLANOBIS, K. SHAHI, AND R. K. SYAL, *Solid State Ionics* **44,** 107 (1990).

55. C. C. LIANG, *J. Electrochem. Soc.* **120,** 1289 (1973).

56. K. SHAHI AND J. B. WAGNER, JR., *Phys. Rev.* **23,** 6417 (1981).

57. K. SHAHI AND J. B. WAGNER, JR., *J. Phy. Chem. Solids* **43,** 713 (1982).

58. K. SHAHI AND J. B. WAGNER, JR., *Solid State Ionics* **12,** 511 (1984).

59. S. R. SAHAYA PRABAHARAN AND P. MUTHUSUBRAMANIAN, "Proc. 3rd Int. Sym. on Solid State Physics, Sri Lanka, 1991," in press.

60. M. A. K. L. DISSANAYAKE, M. A. CAREEM, P. W. S. K. BANDARANAYAKE, R. P. GUNAWARDANE, AND C. N. WIJAYASEKERA, *Solid State Ionics* **40/41,** 23 (1990).

61. M. A. K. L. DISSANAYAKE AND B. E. MELLANDER, *Solid State Ionics* **21,** 279 (1986).

62. M. A. K. L. DISSANAYAKE AND M. A. CAREEM, *Solid State Ionics* **28–30,** 1093 (1988).

63. T. JOW AND J. B. WAGNER, JR., *J. Electro. Chem. Soc.* **126,** 1963 (1979).

64. S. PACK, *in* "Electrochemical Soc. Meeting," Abstract, Los Angeles (1979).

65. J. C. WANG AND N. J. DUDNEY, *Solid State Ionics* **18/19,** 112 (1986).

66. J. MAIER, *Ber. Bunsenges. Phys. Chem.* **89,** 355 (1985).

67. J. MAIER, *J. Phys. Chem. Solids* **46,** 309 (1985).

68. N. F. UVAROV, V. P. ISUPOV, V. SHARMA, AND A. K. SHUKLA, *Solid State Ionics* **51,** 41 (1992).

69. D. G. AST, *Phys. Rev. Lett.* **32,** 1042 (1974).

70. M. F. BELL, M. SAYER, D. S. SMITH, AND P. S. NICHOLSON, *Solid State Ionics* **9/10,** 731 (1983).

71. A. BUNDE, W. DIETERICH, AND E. ROMAN, *Solid State Ionics* **18/19,** 147 (1986).

72. R. J. FRIAUF, *in* "Physics of Electrolytes" (J. Hladik, Ed.), Vol. 1, Academic Press, London (1972).

73. E. A. SECCO, *Solid State Ionics* **28–30,** 168 (1988).

74. J. MAIER, *Ber. Bunsenges. Phys. Chem. Solids* **90,** 29 (1986).

75. J. B. PHIPPS AND D. H. WHITMORE, *Solid State Ionics* **9/10,** 123 (1983).

76. J. MAIER, *Ber. Bunsenges. Phys. Chem. Solids* **88,** 1057 (1984).

77. B.-E. MELLANDER AND D. LAZARUS, *Phys. Rev. B* **31,** 10, 6801 (1985).

78. C. A. ANGELL, *Solid State Ionics* **9/10,** 3 (1983); **18/19,** 72 (1986).